

# Effect of length and geometry on the highest occupied molecular orbital-lowest unoccupied molecular orbital gap of conjugated oligomers: An analytical Hückel model approach

Alexander Onipko<sup>a)</sup>

*Department of Physics and Measurement Technology, Linköping University, S-581 83 Linköping, Sweden*

Yuriy Klymenko

*Space Research Institute, Kiev 252022, Ukraine*

Lyuba Malysheva

*Bogolyubov Institute for Theoretical Physics, Kiev 252143, Ukraine*

(Received 24 June 1996; accepted 5 August 1997)

It is shown that the asymptotic behavior of the highest occupied molecular orbital-lowest unoccupied molecular orbital (HOMO-LUMO) gap of conjugated oligomers of types  $M-(M)_{N-2}-M$  and  $M-(M)_{N-2}-M_1$  with  $M = M_1-M_2$ , where  $M$ ,  $M_1$ , and  $M_2$  are alternant but otherwise arbitrary monomers described by the Hückel Hamiltonian, is ruled by the law  $\Delta_{HL}(N) = \Delta_{HL}(\infty) + \text{const} \cdot N^{-2}$ . On this basis we suggest an approximate expression for the HOMO-LUMO gap as a function of oligomer length, that is exact for minimal- and infinite-length oligomers. Two parameters of this function determine the dependence of  $\Delta_{HL}(N)$  on the oligomer geometry. By comparing the proposed approximation with the exact model results for oligomers of polyene, polyparaphenylene (PPP), and polyparaphenylenevinylene (PPV) (some experimental data and results of more elaborate calculations have been also used for this purpose) the proposed approximation is proven to give a useful estimate of the conjugation length and geometry effect on the HOMO-LUMO gap of the molecules under consideration. Applying our approach to PPP and PPV oligomers, we rederive the geometry effects on the PPP band gap reported previously (however, an important point is taking end effects into account) and predict that the HOMO-LUMO gap of PPV decreases with the increase of the quinoid character of the backbone geometry much more strongly, as compared with PPP. The band gap closing in the infinite chain limit as well as the problem of the existence of discrete in-gap states were also examined, and this analysis has resulted in the formulation of general conditions of the occurrence of the above mentioned situations. Applied to the polymers (infinite oligomers), these conditions allow one to decide whether the gap closing or the existence of in-gap states is possible under the given  $\pi$  electronic structure of monomer. Since the conditions obtained are expressed in terms of the monomer Green function only, they provide a simple and efficient tool with which to search for new polymer materials with the band gaps desired. © 1997 American Institute of Physics. [S0021-9606(97)01742-X]

## I. INTRODUCTION

Conjugated polymer based materials are the subject of continuing experimental and theoretical interest stimulated by the possibility of fabricating efficient polymeric conductors, battery electrodes, light emitting diodes and using them for other applications. The electronic properties of these materials are determined by a number of factors among which the architecture and length of the basic structural components—conjugated oligomers—play a significant if not a decisive role. The dependence of the gap between the highest occupied molecular orbital (HOMO) and the lowest unoccupied molecular orbital (LUMO) on the oligomer length and geometry of molecule is not only of fundamental importance, it is one of the key issues to be considered in designing new polymeric materials, in particular, those with large optical response.<sup>1</sup>

Finding this dependence starting from first principles is an extremely difficult task. The knowledge accumulated thus far due to established numerical calculations is therefore, far from enough for rationalizing existing experimental data. At the same time, it has been convincingly demonstrated that the Hückel model with parameters taken either from experiment or from more elaborate theories can serve as a powerful tool for examining general properties of the  $\pi$  electronic structure such as its dependence on the oligomer backbone geometry,<sup>2,3</sup> end groups and oligomer length.<sup>4-7</sup> As an example, an appropriately parameterized Hückel model not only quantitatively reproduces the  $1^1B_u$  0-0 absorption energies for a number of well defined polyene oligomers,<sup>4</sup> but it also behaves reasonably in the long chain limit and thus allows one to derive information about the conjugation length distribution in long polyenes.<sup>8,9</sup>

Thus, it appears that, even in the case of polyenes, where the applicability of the one-particle approximation has been repeatedly criticized,<sup>10,11</sup> one-particle models have proved to

<sup>a)</sup>Electronic mail: alex@ifm.liu.se

be of significant predicting power at both the qualitative and quantitative levels. However, it must be stressed that because of its simplifications of real molecules the Hückel model fails to reproduce the ordering of polyene excited singlet states observed experimentally,<sup>12</sup> which can be explained by inclusion of electron-electron correlation effects,<sup>13</sup> and this is not the only indication of the restricted applicability of the classic one-particle approximation to linear conjugated molecules. So, on the one hand, an appropriately parameterized Hückel model can be adequate for the description of dipole bands of conjugated oligomers and, in particular, the gap associated with the lowest dipole allowed transition. On the other hand, the results obtained in the framework of this model must be used with a good deal of precaution. Therefore, we are not saying that our conclusions do pretend to give a satisfactory explanation of the full  $\pi$  electronic structure of this type of molecules.

Here we put most of the emphasis on an analytical analysis of the dependence of the HOMO-LUMO gap on the oligomer length and parameters associated with the  $\pi$  electronic structure. This is a part of the strategy<sup>6,7</sup> aimed at examining optical and electrical properties of conjugated oligomers by analytical methods in such detail that are almost impossible to obtain by qualified numerical calculations in a reasonable amount of time. Note in this connection that the problem of a theoretical description of the excitation energy versus molecule length dependence has been repeatedly addressed in the case of polymethine dyes (see, e.g., Ref. 5 and references therein) but we are not aware of any successful attempt that suggests such a dependence for conjugated oligomers consisting of monomers other than a methine group mimicked by a one-level atom.

The main motivation of this work was, then, to find a simple analytical expression of the dependence of the HOMO-LUMO gap  $\Delta_{HL}$  on oligomer length  $N$ . As will be shown below, for a wide class of linear conjugated molecules a quite accurate theoretical estimate of  $\Delta_{HL}(N)$  at any value of  $N$  can be obtained by using only two limiting values of this quantity, namely,  $\Delta_{HL}(2)$  and  $\Delta_{HL}(\infty)$  provided the highest valence and the lowest conduction  $\pi$  electron bands remain separate in the limit  $N \rightarrow \infty$ , and there are no discrete levels in the band gap. The analysis of the band gap closing and of the appearance of in-gap discrete states caused by end effects has led us to a formulation of general conditions (obtained in the one-particle approximation) that relate the above mentioned peculiarities of the  $\pi$  electron spectrum of infinite oligomers to certain properties of the monomer Green function. These conditions, which have far ranging implications regarding forbidden zones in the  $\pi$  electron spectrum, are specified for the HOMO-LUMO gap of PPP and PPV oligomers. In the latter, explicit equations that determine the  $\pi$  electron spectrum of  $N=2$  and  $N=\infty$  oligomers (and hence, values of  $\Delta_{HL}(2)$  and  $\Delta_{HL}(\infty)$ ) have also been derived.

In Sec. II, we specify equations that give the formal basis of this discussion. In Sec. III, we suggest and justify an appealing and simple analytical formula that describes suffi-

ciently well the dependence of the HOMO-LUMO gap on the oligomer length and monomer geometry. Proof of the asymptotic behavior  $\Delta_{HL}(N) - \Delta_{HL}(\infty) \sim N^{-2}$  (given in Appendix A), which is reproduced by the approximate formula, is one of the central, but not the only new, results of this article. In Sec. IV, the proposed approximation is compared with exact model dependences  $\Delta_{HL}(N)$  obtained for oligomers of polyene, quinoid and aromatic forms of polyparaphenylene (PPP) and polyparaphenylenevinylene (PPV). Parallel to this, a number of new analytical relations for these oligomers is presented and used in the discussion of their electronic properties. Section V gives a synopsis of the most important results that were obtained. Some mathematical details, that are essential for the understanding and application of these results are presented in Appendixes A–C.

## II. BASIC EQUATIONS

As is already known,<sup>14–16</sup> in the Hückel theory of  $\pi$  electrons<sup>17</sup> the eigenvalue problem for an arbitrary conjugated oligomer, a sequence of a finite number  $N$  of covalently linked monomers  $M, M-M-\dots-M$ , can be reduced to the solution of a set of two transcendent equations,

$$f_1(E) = 2 \cos \xi, \quad (1)$$

$$f_2(E) = \frac{\sin(N\xi)}{\sin((N-1)\xi)}.$$

The first of these equations determines the dependence of the  $\pi$  electron energy  $E = E_\mu(\xi)$  in the  $\mu$ th band (the number of which is equal to or less than the number of  $\pi$  centers in monomer  $M$ ) on the quantum number  $\xi$ , while solutions to the second equation, where  $E$  is replaced by  $E_\mu(\xi)$ , determine values of  $\xi$  within each band.

The set just referred to is completely equivalent to the initial eigenvalue problem except those  $\pi$  electron states, whose wave functions have nodes at the binding sites, i.e., left ( $l$ ) and right ( $r$ ) atoms of  $M$  connected via the electron transfer resonance interaction with  $r$  and  $l$  binding atoms of the left and right neighboring monomers, respectively. Such energies (subject to the solution of a much more simple eigenvalue problem for an isolated monomer) are not affected by the intermonomer interaction and therefore they do not depend on the oligomer length. It is also worth mentioning that the number of real solutions for  $\xi$ , which correspond to the given dependence  $E_\mu(\xi)$  can be equal to  $N$  or less. In the latter case, there exist  $\pi$  electron levels genetically connected with, say, the  $\mu$ th band but, with energies lying within intervals  $E_{\mu-1}^{max}(\xi) < E < E_{\mu}^{min}(\xi)$  or/and  $E_{\mu}^{max}(\xi) < E < E_{\mu+1}^{min}(\xi)$ , the so-called local levels (see below).

There is a vast variety of linear conjugated molecules covered by the structural formulae  $M-M-\dots-M$ , which implies that monomers are connected with each other via a chemical bond. Usually, this is a C-C bond. However, often, to form an oligomer, monomers are connected not directly to but through a certain atomic group. A typical example is oligomers of polyparaphenylenevinylenes, where phenyl

rings ( $M_1$ ) are connected through a vinylene group ( $M_2$ ). Such oligomers can be modeled by a regular chain with an end defect:  $M-M-\dots-M-M_1$ , where  $M = M_1-M_2$ . (The synthesis of novel oligo(phenylenevinylenes) was reported several years ago.<sup>18</sup>) Using solid state terminology, the latter structure can be considered as a finite one-dimensional crystal with elementary cells  $M_1-M_2$  and one defect cell  $M_1$  at its end. Because of the formal similarity of the structure of these two types of oligomers, both  $M-M-\dots-M$  and  $M_1-M_2-M_1-\dots-M_2-M_1$  are included in the present context.

There can be several forms of equations that are equivalent to the initial Schrödinger problem with the Hückel Hamiltonian used to describe conjugated oligomers. Their particular form depends on the method of derivation. This can be, for example, the transfer matrix,<sup>14</sup> polynomial matrix<sup>15</sup> method, or ones similar to these.<sup>16</sup> To make these equations more explicit physically, it seems preferable to use the Green function formalism that proved to be extremely efficient in the analysis of the  $\pi$  electron spectrum of linear conjugated molecules.<sup>5-7</sup> As will be seen later, the representation of functions  $f_1(E)$  and  $f_2(E)$  in terms of certain components of the Green function for an isolated monomer is in many respects useful for understanding the interrelation between the monomer and oligomer  $\pi$  electronic structures.

Omitting technical details, for oligomers of the type  $M-M-\dots-M$  we can write<sup>19(a)</sup>

$$f_1(E) = \frac{1}{G_{l,r}^M(E)} [1 - G_{l,l}^M(E)G_{r,r}^M(E) + (G_{l,r}^M(E))^2], \quad (2)$$

$$f_2(E) = G_{l,r}^M(E),$$

where  $G_{j,j'}^M = \beta \langle j | (E - H^M)^{-1} | j' \rangle$ ,  $H^M$  is the Hamiltonian operator of monomer  $M$ ;  $|j\rangle$ ,  $j = l, r$ , is the binding site atomic orbital; and  $\beta$  is the resonance interaction energy between monomers.

For oligomers of type  $M-M-\dots-M-M_1$ , where  $M = M_1-M_2$ , the eigenvalue problem can also be reduced to set (1), where  $N$  corresponds to the number of monomers  $M_1$ , and functions  $f_1(E)$  and  $f_2(E)$  have the form<sup>19(b)</sup>

$$f_1(E) = \frac{1}{G_{l,r}^{M_1}(E)G_{l,r}^{M_2}(E)} \{1 - G_{l,l}^{M_1}(E)G_{r,r}^{M_2}(E) - G_{l,l}^{M_2}(E)G_{r,r}^{M_1}(E) + [G_{l,l}^{M_1}(E)G_{r,r}^{M_1}(E) - (G_{l,r}^{M_1}(E))^2][G_{l,l}^{M_2}(E)G_{r,r}^{M_2}(E) - (G_{l,r}^{M_2}(E))^2]\}, \quad (3)$$

$$f_2(E) = -\frac{G_{l,r}^{M_1}(E)}{G_{l,r}^{M_2}(E)} [G_{l,l}^{M_2}(E)G_{r,r}^{M_2}(E) - (G_{l,r}^{M_2}(E))^2].$$

Note that the above equations coincide with the definitions of functions  $f_1(E)$  and  $f_2(E)$  given in Eq. (2), if ‘‘connecting’’ group  $-M_2-$  is equivalent to the C-C bond. Indeed, for a non-alternating chain of  $N_2$  carbons the diagonal and non-diagonal Green function components are equal to

$G_{l,l}^{M_2}(E) = G_{r,r}^{M_2}(E) = \sin(\xi N_2) / \sin(\xi(N_2 + 1))$  and  $G_{l,r}^{M_2}(E) = \sin \xi / \sin(\xi(N_2 + 1))$ , respectively ( $E$  and  $\xi$  are interrelated by Eq. (1)). Obviously,  $-M_2 = -C-C$ , if we formally set  $N_2 = 0$ , i.e.,  $G_{l,l}^{M_2}(E) = 0$  and  $G_{l,r}^{M_2}(E) = 1$  and thus, in this case Eq. (3), where  $M_1 = M$ , coincides with Eq. (2).

Equation (1) together with explicit expressions for  $f_1(E)$ ,  $f_2(E)$  and for the Green function matrix elements  $G_{l,l}^M(E)$ ,  $G_{r,r}^M(E)$ ,  $G_{l,r}^M(E)$  (where  $E$  is expressed in units  $\beta$ , and the Coulomb integral for carbon atom is set equal to zero) provide the exact description of the  $\pi$  electron spectrum of oligomers of types  $M-M-M-\dots-M$  and  $M-M-\dots-M-M_1$ . In the present context, the term ‘‘exact’’ means that this spectrum is calculated exactly on the basis of the Hückel model. It is also a good time to recall that, as mentioned above, the solutions to Eq. (1) should be supplemented by  $N$ -fold degenerated eigenvalues which are not affected by the inter-monomer interaction, see, for more details, Ref. 19(a).

### III. ANALYTICAL FORMULAE FOR THE 0-0 $B_u$ TRANSITION ENERGY

Equation (1) determines the dependence of  $\pi$  electron levels on the oligomer length and monomer geometry implicitly. Although finding solutions to this equation is a much more simple task than that one encounters handling the initial Schrödinger problem, it is still too complicated to be used for a quick analysis of the above mentioned dependence. Therefore, it is highly desirable to obtain at least an approximate analytical expression for the dependence of the HOMO-LUMO gap (denoted below as  $\Delta_{HL}(N)$ ) on the oligomer length  $N$ .

From the mathematical point of view it is, in principle, possible to derive such a dependence in the long chain limit. However, one can expect that, if applied to shorter oligomers, it would fail to reproduce  $\Delta_{HL}(N)$ . To make the approximate dependence  $\Delta_{HL}^{approx}(N)$  applicable to oligomers of an arbitrary length, we set

$$\Delta_{HL}^{approx}(2) = \Delta_{HL}(2), \quad (4)$$

$$\Delta_{HL}^{approx}(\infty) = \Delta_{HL}(\infty).$$

Of course, an approximation based on the above equations cannot pretend to give a precise description of  $\Delta_{HL}(N)$  at intermediate values of  $N$ . However, as is demonstrated in Sec. IV, such an approximation provides a reasonable quantitative estimate of  $\Delta_{HL}(N)$  at any length and, more important, it reflects the main tendencies of HOMO-LUMO gap dependence on the monomer structure and on the particular form of the oligomers.

Except for some special cases the behavior of the HOMO-LUMO gap at large  $N$  is described by  $\Delta_{HL}(N) = \Delta_{HL}(\infty) + \text{const} \cdot N^{-2}$ . This law, which is proved in Appendix A, is a direct consequence of the fact that in a sufficiently long but finite chain deviation of the band-edge values of  $\xi$  from their limiting values 0 and  $\pi$  attained in the limit  $N \rightarrow \infty$  is proportional to  $N^{-1}$ . Excluding the aforementioned special cases connected with the possibility of band

joining or the existence of in-gap local states, as discussed in Appendix B, a function, that has the minimal number of adjustable parameters and coincides with the exact values of  $\Delta_{HL}(N)$  at  $N=2$  and  $N=\infty$  can be taken in the form

$$\Delta_{HL}^{approx}(N) = A - B \cos\left(\frac{\pi}{N+1}\right), \quad (5)$$

where constants  $A$  and  $B$  are defined as

$$A = 2\Delta_{HL}(2) - \Delta_{HL}(\infty)$$

and

$$B = 2[\Delta_{HL}(2) - \Delta_{HL}(\infty)]. \quad (6)$$

It is worth mentioning that, formally, Eq. (5) describes the band-bottom energy of an excess electron in a monoatomic chain consisting of  $N$  atoms, where the electron site energy is equal to  $A$ , and the intersite resonance interaction—to  $-B/2$ . As seen from Eq. (6) neither of these meanings is applicable if the dependence (5) is used to fit the excitation energy of the 0-0 dipole transition of oligomers.

To calculate  $\Delta_{HL}^{approx}(N)$  for all  $N$ , one needs to know the exact values of  $\Delta_{HL}(N)$  only for the shortest ( $M-M$  or  $M_1-M_2-M_1$ ) and infinite oligomers. For  $N=2$  we have instead of (1)

$$f_1(E) - f_2(E) = 0, \quad (7)$$

and in the limit  $N \rightarrow \infty$  the edge energies of  $\pi$  electron bands are subject to solution of the upper equation of set (1) with  $\xi$  replaced by 0 or  $\pi$ , i.e.,

$$f_1(E) \pm 2 = 0, \quad (8)$$

where the choice of sign depends on the particular structure of the monomer.

In accordance with their definition, the quantities  $\Delta_{HL}(2)$  and  $\Delta_{HL}(\infty)$  are determined by their solutions to Eq. (7) (for the former) and Eq. (8) (for the latter) which correspond to the HOMO and LUMO levels. Only the smallest roots of the above equations are needed if one deals with alternant oligomers that have an even number of identical  $\pi$  centers in their building blocks—monomers.

Finally, in many cases of interest the expressions for the Green function matrix elements appearing in the definitions of  $f_1(E)$  and  $f_2(E)$  can be obtained in an explicit form, as is illustrated by representative examples given in Appendix B. Then, Eq. (5) makes “visible” not only the dependence of the HOMO-LUMO gap on oligomer length but also on parameters which are directly related to the monomer geometry.

Thus, taking into account the minor restrictions indicated above and specified in Appendix B, Eqs. (5)–(8) suggest an appealingly simple procedure that allows one to examine in great detail the dependence of the HOMO-LUMO gap (and hence of the related quantities measured experimentally, e.g., the 0-0 transition frequency of the lowest dipole allowed excitation) on the basic parameters of conjugated oligomers. An example of such an analysis is given in Sec. IV, where we turn to a comparison of the proposed analytical formulae

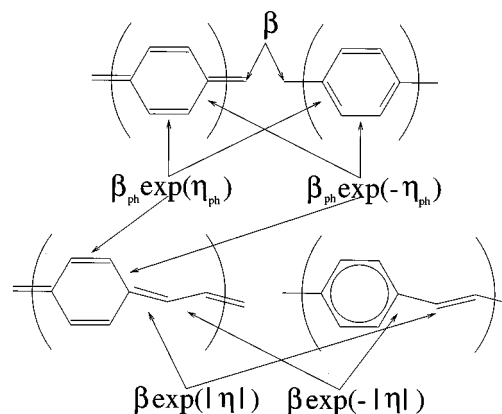


FIG. 1. Quinoid (left) and benzenoid (right) geometries of PPP (upper) and PPV (lower) oligomers. The arrows indicate the resonance integrals associated with different C-C bonds.

with the exact model results for (alternant) oligomers of polyene, polyparaphenylene, and polyparaphenylenevinylene. The Green function matrix elements needed for this are defined in Eqs. (B7)–(B11). The calculation of the limiting values of the HOMO-LUMO gap,  $\Delta_{HL}(2)$  and  $\Delta_{HL}(\infty)$ , which determines constants  $A$  and  $B$  in Eq. (5), is discussed in Appendix C.

#### IV. COMPARISON OF APPROXIMATE RESULTS WITH PREDICTIONS OF THE HÜCKEL MODEL

We now present the results of calculations of the HOMO-LUMO gap versus oligomer length dependence that were performed for the above mentioned oligomers using both the exact definition of  $\Delta_{HL}(N)$  from Eq. (1) and an approximate one given in Eq. (5). The aim of these calculations is twofold. On the one hand, they demonstrate the accuracy of the proposed approximate analytical description compared with the exact model results and show that the dependence  $\Delta_{HL}^{approx}(N)$  can be used, in many cases to the least length, for a quick and reliable estimate of the HOMO-LUMO gap and variations of this quantity by changes in the number of monomers and changes in their geometry. On the other hand, these calculations make the relative role and microscopic origins of major factors that determine the HOMO-LUMO gap value apparent and can therefore be helpful in interpreting relevant experimental data.

A commonly accepted practice, a particular geometry of oligomers can be taken into account by relating non-equivalent C-C bonds to different resonance integrals. In the oligomers under consideration these are, in polyenes, the integrals associated with the double ( $\beta_{C=C} = \beta \exp \eta$ ) and single ( $\beta_{C-C} = \beta \exp(-\eta)$ ) C-C bonds; in PPPs, similar notations, namely,  $\beta_{ph} \exp(\pm \eta_{ph})$ , are used for the same bonds in a phenyl ring, while  $\beta$  refers to the resonance interaction between the rings, see Fig. 1; correspondingly, in PPVs,  $\beta_{ph} \exp(\pm \eta_{ph})$  and  $\beta \exp(\pm \eta)$  distinguish double (+) from single (−) bonds within and between the rings, respectively. By convention, we make  $\eta$  positive (negative) for an aro-

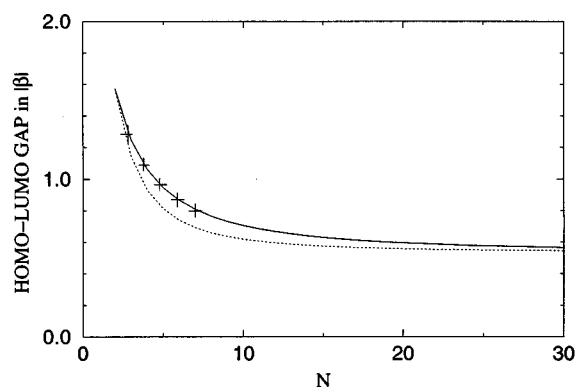


FIG. 2. HOMO-LUMO gap vs number of double bonds in polyene oligomers. Solid line—Eq. (1); dotted line—Eq. (5);  $\eta=0.1333^4$ ; crosses—experimental data of Ref. 4.

matic (quinoid) structure of PPV. Thus, being expressed in units of  $|\beta|$ , the HOMO-LUMO gap, in addition to its dependence on  $N$ , is also a function of  $\eta$  for polyenes, of  $\eta_{ph}$  and  $\gamma = \beta_{ph}/\beta$  for PPPs, and of  $\eta_{ph}$ ,  $\eta$ , and  $\gamma$  for PPVs.

According to experimental data accumulated for PPP,<sup>3,20</sup>  $\eta_{ph} \approx 0.01$ ,  $|\gamma - 1| \approx 0.1$ , and it is reasonable to assume that  $|\eta| \approx 0.1$ . The parameters used in our calculations include the above indicated values, as well as those of intermediate and extreme aromatic (i.e., benzenoid) and quinoid-like geometries. For PPP and PPV the latter are associated with the structures shown in Fig. 1. The transition from one type of geometry to another includes passing the equalized bond model ( $\gamma = 1$ ,  $\eta_{ph} = \eta = 0$ ). For this reason in the discussion of the evolution of the HOMO-LUMO gap in response to changes of the backbone geometry, it is instructive to use this model as a reference point. The dependences  $\Delta_{HL}(N)$  which correspond to the equalized bond model are shown in Fig. 3 by bold-faced curves. The solid lines in Figs. 2 and 3 represent the results of exact model calculations, and the dotted lines are the approximation of Eq. (5).

For each type of oligomer geometry we are interested in the sensitivity of the HOMO-LUMO gap with respect to changes in the ratio of the resonance interaction within monomers and between monomers (this can be traced by

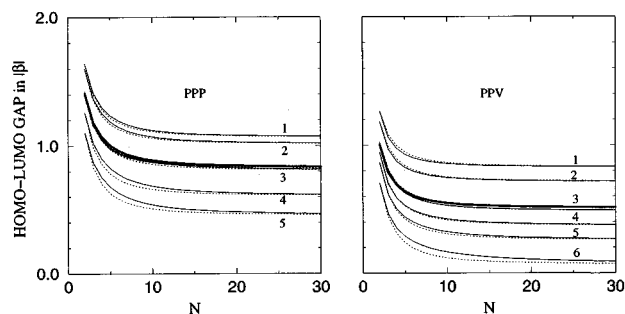


FIG. 3. HOMO-LUMO gap vs number of monomers in oligomers of poly-paraphenylene and polyparaphenylenevinylene. Solid lines—Eq. (1); dotted lines—Eq. (5); the labeling of the curves corresponds to the labeling of the rows in Table I; bold-faced curves—equalized bond model.

varying parameter  $\gamma$ ), and to changes in the difference between single and double C-C bonds within monomers (parameter  $\eta_{ph}$ ) and between monomers (parameter  $\eta$  for PPVs only). In Fig. 3, the dependences  $\Delta_{HL}(N)$  displayed above and below bold-faced curves illustrate how large the increase or decrease of the HOMO-LUMO gap can be under possible changes towards an aromatic or quinoid character of the oligomer geometry.

The dependence  $\Delta_{HL}(N)$  for polyenes, where both the parameterization of the Hückel Hamiltonian and experimental data are borrowed from Ref. 4, is presented as an illustration of the high accuracy of the given model (solid line) in reproducing the established results (crosses) on the 0-0  $B_u$  band excitation energy versus chain length. The excellent agreement between theory and experiment obtained in Ref. 4 encourages us to apply the same simple model to more complex molecules, such as oligomers of PPP and PPV discussed in the later portion of this article. However, the model predictions coinciding with the observed variation of the  $1^1A_g \rightarrow 1^1B_u$  transition frequency for a restricted number of polyenes (with 3–7 double bonds) cannot be considered as a proof of validity for the Hückel model in the long chain limit. To our knowledge, its validity has been neither confirmed nor rejected.

As seen from Figs. 2 and 3, in the limit  $N \rightarrow \infty$ , the dependence  $\Delta_{HL}(N)$  for oligomers of polyene, PPP, and PPV (and very likely most of conjugated oligomers; see Sec. III and Appendixes A and B) follows the universal behavior  $\Delta_{HL}(N) - \Delta_{HL}(\infty) \sim N^{-2}$  which coincides with that implied by Eq. (5). The approximation (5) also agrees reasonably well with the exact model calculations of the HOMO-LUMO gap as a function of chain length and other characteristic parameters of the oligomer. A number of calculations performed on the basis of Eq. (1) and compared with Eq. (5), which cover in excess all the values of the characteristic parameters that are considered reasonable for PPP and PPV oligomers (Table I and Fig. 3 represent part of the parameters used) show that, despite some lack of quantitative accuracy, the suggested approximation reliably reproduces the main trends of the gap behavior. But in the strict sense of the word, Eq. (5) fails to reproduce function  $\Delta_{HL}(N)$  at short and intermediate lengths, where the use of exact equations (1) is preferable.

So, taking into account the appealing simplicity of Eq. (5) and its increasing accuracy for longer oligomers, this approximation can be suggested as a quick alternative to Eq. (1) for carrying out a preliminary analysis, especially for large  $N$ , when exact calculations require an ever-increasing amount of time.

Now we turn to a comparison of previous with our (in certain aspects more detailed) results for PPP oligomers and to conclusions concerning PPV oligomers that have not been discussed thus far in the present context.

TABLE I. Constants  $A$  and  $B$  (in units  $|\beta|$ ) which determine the dependence of HOMO-LUMO gap on the number of monomers in oligomers of polyene, polyparaphenylene, and polyparaphenylenevinylene. Data from the labelled rows were used in the calculations shown in Fig. 3.

Oligomer	$\gamma$	$\eta_{ph}$	$\eta$	$\Delta_{HL}(2)$	$\Delta_{HL}(\infty)$	$A$	$B$
Polyene			0.1333 <sup>a</sup>	1.572	0.535	2.609	2.074
PPP							
all equal bonds	1.0	0.00		1.410	0.828	1.992	1.164
benzenoid form	1.0	0.10		1.446	0.878	2.014	1.136
	<sup>2</sup> 1.1	0.00		1.600	1.013	2.187	1.174
	<sup>1</sup> 1.1	0.10		1.641	1.066	2.216	1.150
quinoid form	<sup>5</sup> 1.0	0.10		1.102	0.456	1.748	1.292
	<sup>3</sup> 1.1	0.05		1.425	0.807	2.043	1.236
	<sup>4</sup> 1.1	0.10		1.259	0.608	1.910	1.302
PPV							
all equal bonds	1.0	0.00	0.00	1.009	0.508	1.510	1.002
benzenoid form	1.0	0.00	0.10	1.164	0.728	1.600	0.872
	1.1	0.00	0.00	1.105	0.600	1.610	1.010
	<sup>2</sup> 1.1	0.00	0.05	1.187	0.715	1.659	0.944
	<sup>1</sup> 1.1	0.00	0.10	1.270	0.829	1.711	0.882
quinoid form	1.0	0.00	-0.10	0.860	0.287	1.433	1.146
	<sup>6</sup> 1.0	0.10	-0.10	0.706	0.068	1.344	1.276
	<sup>3</sup> 1.1	0.00	-0.05	1.024	0.485	1.563	1.078
	<sup>4</sup> 1.1	0.00	-0.10	0.946	0.370	1.522	1.152
	1.1	0.05	-0.05	0.941	0.372	1.510	1.138
	<sup>5</sup> 1.1	0.05	-0.10	0.867	0.258	1.476	1.218
	1.1	0.10	-0.10	0.787	0.144	1.430	1.286

<sup>a</sup>From Ref. 4.

The curves for PPP oligomers reveal the same dependence of the HOMO-LUMO gap on the geometry parameters of the molecule backbone that was first predicted by Brédas<sup>2</sup> and investigated in more detail by Brédas *et al.*<sup>20</sup> and by Ambrosch-Draxl *et al.*<sup>3</sup> In the papers cited periodic boundary conditions were used and, thereby, the finite length and the existence of ends in real molecules were neglected. The present calculations also answer next question, To what extent do geometry effects depend on oligomer length?

Figure 3 shows that in both PPP and PPV oligomers, and independent of their particular geometry, the HOMO-LUMO gap increases with the increase of  $\gamma$ , that is, with the relative decrease of intermonomer resonance interaction which can be caused by the decrease of C-C bond strength between the phenyl rings due to, e.g., alternate twisting the rings relative to each other. (To recap, since  $\Delta_{HL}$  is expressed in units  $|\beta|$ , the increase (decrease) of  $\Delta_{HL}$  with the increase (decrease) of  $\gamma$  illustrated in Fig. 3 is actually partly cancelled if changes in the latter's quantity are caused exclusively by the decrease (increase) of  $|\beta|$ .)

In a sense, the result just pointed out is trivial since it reflects the tendency of  $E_{LUMO}^M$  towards the monomer LUMO energy  $E_{LUMO}^M$  in response to weakening of intermonomer interaction. Obviously, the effect indicated can be considered as a general property of this kind of oligomer. In contrast, the dependence on  $\eta_{ph}$  (non-equivalence of single and double C-C bonds within the ring) is substantially different in the benzenoid and quinoid-like structures: the increase of  $\eta_{ph}$  causes a weak increase of  $\Delta_{HL}$  in the former, and a strong decrease of  $\Delta_{HL}$  in the latter. In other words, to the linear approximation in  $\eta_{ph}$  the HOMO-LUMO gap of aromatic structured PPP oligomers is practically insensitive to whether C-C bonds within phenyl rings are assumed to be equalized or formally alternated, whereas in the case of the quinoid structure of the ring, the difference between the single and double bonds has a dramatic effect on the band gap.

The origin of this effect becomes clear if we consider the dependence of  $|E_{LUMO}^M|$  ( $=|E_{HOMO}^M|$  since the Coulomb integral of carbon atom is set equal to zero) on  $\eta_{ph} \ll 1$ . Expanding the minimal positive poles of Green functions of the phenyl ring in aromatic and quinoid conformations given in Eqs. (B8) and (B9) in powers of  $\eta_{ph}$ , we obtain to the lowest power of the small parameter

$$|E_{LUMO}^M| \approx \gamma(1 + 2\eta_{ph}^2), \quad \text{aromatic form,} \quad (9)$$

$$|E_{LUMO}^M| \approx \gamma\left(1 - \frac{5}{3}\eta_{ph}\right), \quad \text{quinoid form.}$$

The behavior of  $\Delta_{HL} = 2|E_{LUMO}^M|$  as a function of  $\eta_{ph}$  is a reflection of the above dependences. Of course, in oligomers  $|E_{LUMO}^M|$  acquires a quantitatively different dependence on  $\eta_{ph}$  but qualitatively it remains the same. As shown in Appendix C, in the long chain limit this dependence can be expressed analytically for both benzenoid and quinoid forms of PPP. Precisely, for the former we have (in units  $|\beta|$ )

$$\Delta_{HL}(\infty) = 2\sqrt{Z_{min} + \gamma^2(2\cosh(2\eta_{ph}) - 1)}, \quad (10)$$

where  $Z_{min}$  is the minimal (in the absolute value) root of equation

$$Z^3 - (1 + 3\gamma^2)Z^2 - 4\gamma^2[\gamma\cosh(2\eta_{ph}) + \sinh^2\eta_{ph}]Z + 4\gamma^4\sinh^2\eta_{ph} = 0, \quad (11)$$

and for the latter

$$\Delta_{HL}(\infty) = \sqrt{2} \sqrt{1 + \gamma^2 \exp(2\eta_{ph}) + 4\gamma^2 \exp(-2\eta_{ph}) - [1 - \gamma^2 \exp(2\eta_{ph})] \sqrt{1 + 8\left(\frac{\gamma \exp(-\eta_{ph})}{1 - \gamma \exp \eta_{ph}}\right)^2}}. \quad (12)$$

To describe the aromatic and quinoid PPV structures, we use for the former the equalized bond model of the phenyl ring which, as shown above, is accurate to the linear order in  $\eta_{ph}$ . Then, the HOMO-LUMO gap in the limit  $N \rightarrow \infty$  is determined by  $\Delta_{HL}(\infty) = 2E_{min}$ , where  $E_{min}$  is the smallest (in the absolute value) root of the polynomial (C10), where  $\xi$  is set equal to  $\pi$  (see Appendix C),

$$E^6 - [3\gamma^2 \exp(-2\eta_{ph}) + 2(\gamma^2 \cosh(2\eta_{ph}) + \cosh(2\eta)) + \exp(-2\eta)]E^4 + \{\exp(-4\eta) + \gamma^2[4\exp(-2\eta_{ph}) \times (\gamma^2 \exp(-2\eta_{ph}) + 2\cosh(2\eta)) + \exp(2\eta_{ph}) \times (2\cosh(2\eta) + \exp(-2\eta))]\}E^2 - \gamma^2[\exp(2\eta_{ph} - 4\eta) + 4\gamma^2 \exp(2\eta - 4\eta_{ph}) - 4\gamma \exp(-(\eta_{ph} + \eta))] = 0. \quad (13)$$

When using the above equation for the benzenoid geometry,  $\eta_{ph}$  should be set equal to zero, and  $\eta > 0$ ; the quinoid geometry implies that  $\eta_{ph} > 0$ , and the sign of  $\eta$  is negative.

Taking into account that for the equalized bond model  $E_{LUMO}^2 \ll 1$  we can solve Eq. (13) approximately, omitting terms of the higher order than  $E^2$ . Thus, for  $|\eta|$ ,  $\eta_{ph} \ll 1$  we have

$$\Delta_{HL}(\infty) \approx 2\gamma \frac{|2\gamma - 1|}{\sqrt{4\gamma^4 + 11\gamma^2 + 1}} \times \left\{ 1 + \left( 2 \frac{2\gamma^2 + \gamma - 1}{(2\gamma - 1)^2} + \frac{\gamma^2 + 2}{4\gamma^4 + 11\gamma^2 + 1} \right) \eta - \left( \frac{8\gamma^2 - 2\gamma - 1}{(2\gamma - 1)^2} - \gamma^2 \frac{8\gamma^2 + 5}{4\gamma^4 + 11\gamma^2 + 1} \right) \eta_{ph} \right\}. \quad (14)$$

Predictions of the above equation are in a good quantitative agreement with exact values of  $\Delta_{HL}(\infty)$  calculated from Eq. (13) and represented in Table I. In particular, Eq. (14) indicates that for  $\gamma = 1$  we have  $\Delta_{HL}(\infty) = 0.5 - (67/32)(\eta_{ph} - \eta)$ , i.e., that in the case of quinoid geometry ( $\eta < 0$ ) the gap decrease in response to the increase of either  $\eta_{ph}$  or  $|\eta|$  has the same rate. For example, the HOMO-LUMO gap at  $\eta_{ph} = 0.1$  and  $\eta = 0$  is equal to that at  $\eta_{ph} = 0$  and  $\eta = -0.1$ . For a more realistic model,  $\gamma \neq 1$  but  $|\gamma - 1| \ll 1$ , the changes of the gap produced by increasing the quinoid character of the phenyl rings in the chain (increase of  $\eta_{ph}$ ) and by increasing the difference between the double and single C-C bonds of the connecting structure (increase of  $|\eta|$ ) are nearly of equal importance.

It is of interest to compare the band gap and its response to the increase of the quinoid character in PPV and PPP. In the long chain limit, the equalized bond model predicts for PPV about a 1.6 times narrower band gap ( $0.508|\beta|$ ) than for PPP that has  $(2(3 - 2\sqrt{2})^{1/2}|\beta| \approx 0.828|\beta|)$ . This is due to the phenylene-vinylene ( $M_1 - M_2$ ) resonance interaction, which lowers the LUMO level of the PPV monomer compared with that of a phenyl ring. Therefore, if the  $\pi$  conjugation does not differ much, it is an intrinsic property of PPV

oligomers that they have a substantially smaller HOMO-LUMO gap compared to PPPs. However, it must be emphasized that this result is valid only under the assumption of an equal degree of conjugation in the PPP and PPV. In the language of the model given, this means that in both polymers the intermonomer resonance interaction is essentially the same, which is not necessarily the case in real materials.

As seen from Fig. 1, the increase of the quinoid character of the backbone of PPP and PPV oligomers is associated with the increase of one ( $\eta_{ph}$ ) and two ( $\eta_{ph}$ ,  $|\eta|$ ) parameters, respectively. Therefore, similar changes in the relative difference between double and single C-C bonds produce a stronger effect on the band gap in PPV than in PPP oligomers; see Table I. In brief, the possibility of obtaining a stronger effect on the HOMO-LUMO gap of PPV by increasing the quinoid character is a consequence of the larger capability of the PPV backbone to change its geometry into a favorable direction.

As was mentioned above, in the infinite chain limit the interrelation between the band gap and the backbone geometry of PPP has been already examined in great detail.<sup>2,3,20</sup> However there is one important question that has not been answered in previous studies; this question concerns the limiting behavior of the band gap as a function of the parameters of the backbone structure. What should be expected if the quinoid character is stronger than that prescribed by values of the parameters used in the present and in previous calculations? For the PPP model this question is of theoretical interest only. But a nearly zero value of the gap obtained for PPV at  $\gamma = 1$ ,  $\eta_{ph} = -\eta = 0.1$  indicates that for this, and probably for some other oligomers, closing of the band gap can be attained or nearly attained. What then are the conditions of zero distance between the highest occupied and the lowest unoccupied levels?

Within the framework of the model given this question is answered here in a quite general form; see Appendix B. For alternant oligomers this answer can be expressed in the form of particularly simple conditions. Namely,  $\Delta_{HL}(\infty) = 0$  if

$$G_{l,l}^M(0)G_{r,r}^M(0) = 0, \quad (15)$$

and

$$|G_{l,r}^M(0)| \geq 1, \text{ for } M - M - \dots - M,$$

$$|G_{l,r}^{M_1}(0)G_{l,r}^{M_2}(0)| \geq 1, \text{ for } M_1 - M_2 - M_1 - \dots - M_2 - M_1, \quad (16)$$

where the sign “=” in Eq. (16) corresponds to the gap closing as a result of band joining, whereas the fulfillment of inequality (16) is the existence of a twofold degenerate local level in the middle of the band gap in the limit  $N \rightarrow \infty$ .

For PPPs and PPVs condition (16) predicts (see Eq. (B12) in Appendix B) that with the increase of the quinoid character of the backbone the highest valence and lowest conduction bands approach each other up to the gap closing. At this point equality (16) is fulfilled. Under a further increase of the quinoid character (reflected in the increase of the non-diagonal component of the monomer Green func-

tion) the bands diverge, but the HOMO and LUMO levels preserve their fixed positions in the middle of the band gap.

For a rough estimate of parameters  $\eta_{ph}$ ,  $\eta$ , and  $\gamma$  we accept Harrison's  $l^{-2}$  rule<sup>21</sup> and set  $\beta_{C-C} \sim l_{C-C}^{-2}$ , where  $l_{C-C}$ , is the C-C bond length. Then, using the data of STO-3G calculations of optimized geometry of 50 mol % sodium doped polyparaphenylene<sup>20</sup> which give  $l_{C-C} - l_{C=C} \approx 0.1 \text{ \AA}$  ( $l_{C=C}$  and  $l_{C-C}$  refer to the C-C bonds that are parallel and inclined to the chain axis, respectively) we determine that the extreme quinoid geometry of the PPP backbone can be characterized by  $\eta_{ph} \approx 0.1$ ,  $\gamma \approx 1.1$ . According to (B12), this set of parameters is far from satisfying the condition of gap closing  $\gamma^{-1} = 2 \exp(-3\eta_{ph})$ . Assuming that upon PPV n-type doping these parameters can reach the same values and that the C-C bond difference between the rings is comparable to that within the rings, i.e.,  $-\eta \approx \eta_{ph} \approx 0.1$ , one comes to the conclusion that the band gap of n-type heavily doped PPV may be about four times smaller than that of PPP with a similar quinoid-like contribution to the electronic structure; see Table I. Just as in the case of PPP, this result is consistent with the condition of gap closing in PPV  $\gamma^{-1} = 2 \exp[-3(\eta_{ph} + |\eta|)]$  which for the given parameters is much closer to fulfillment than the similar condition for PPP. Note that the above very crude estimate does not account for polaronic effects which may even more strongly influence the band gap.<sup>20</sup>

An effective increase of the quinoid-like contribution to the electronic structure of aromatic ring based polymers can also be attained by certain types of substitution as was demonstrated for polythiophene and its derivatives.<sup>22</sup> To examine this possibility, use of the monomer Green function in the way discussed in Appendix B can be especially useful since it allows one to make a preliminary estimate of the substitution effect on the band gap at the monomer level. So, important in this analysis is not numbers but that knowledge of only the monomer Green function can be extremely helpful in making the right choice of monomer to obtain the polymer band gap desired.

## V. CONCLUSIONS

Quantum chemistry aided design of organic polymers<sup>23</sup> implies first of all the ability of a theory at the least possible cost to oversee properties of conjugated oligomers, which are of a fundamental and practical significance, and to show possible ways for their modification. From this point of view we summarize briefly the main findings of the work.

One of the central results is represented by Eq. (5) which shows that the HOMO-LUMO gap of conjugated oligomers, with the exceptions that were specified, tends towards a constant value as the number of monomers increases in accordance with the law  $\Delta_{HL}(N) - \Delta_{HL}(\infty) \sim N^{-2}$  which is in contrast with the  $N^{-1}$  dependence expected from the experience gathered for polymethine dyes.<sup>24,25</sup> In view of the simplified character of the model, this result needs to be confirmed by computational methods.

It was demonstrated that the above mentioned dependence prescribed by the exactly solvable model can be re-

markably well reproduced by approximation (5) in the entire region of the oligomer length thus providing a quick and reliable evaluation of  $\Delta_{HL}(N)$  on the basis of only two parameters  $\Delta_{HL}(2)$  and  $\Delta_{HL}(\infty)$ . Needless to say, the precise theoretical determination of the latter quantities is a much easier task than calculation of the HOMO-LUMO gap at each value of the oligomer length. So the proposed approximation can be efficiently used for a preliminary estimate of the HOMO-LUMO gap dependence as a function of the monomer number and of the parameters of the oligomer backbone structure, and can be used in combination with more elaborate theoretical models. Alternatively, the determination of constants in Eq. (5) from experiment, e.g., from measurements of the 0-0 transition frequency, allows one to draw certain conclusions about the actual microscopic structure of the given oligomer by comparing experimental data with the predictions concerning the HOMO-LUMO gap dependence on parameters of PPP and PPV oligomers made above.

It was shown that the  $\pi$  electronic structure of a monomer is key to understanding the relationship between the oligomer backbone structure and the HOMO-LUMO gap value. In this respect, a determination of the conditions that relate the HOMO-LUMO gap closing in the infinite chain limit with certain properties of the monomer Green function is of special importance from both fundamental and practical points of view. As to the first, this is, at least, not a frequent example when zeros (not poles) of the Green function have direct physical meaning. As to the latter, the conditions obtained allows one to estimate whether or not the narrow (zero) band gap of a designed polymer is realistic by examining the Green function of its monomer.

Possible changes of the PPV band gap with the increase of the quinoid character of the backbone are discussed above in great detail. For this we derived the analytical expression of the band structure as a function of the C-C bond difference within and between phenyl rings, which implies a number of applications. It is shown that under the assumption of an equal degree of conjugation the band gap suppressing effect of the increased quinoid character of PPV is substantially larger than a similar effect predicted previously for PPP. Apart from all this, the result confirms the heuristic power of the conditions of band gap closing derived here and issues a challenge to find the most favorable monomer geometries for obtaining polymeric materials with a small or even zero band gap.

## ACKNOWLEDGMENTS

The authors extend their gratitude to Dr. S. Stafström for critical reading of the manuscript and for valuable comments. This work was supported in part by the Swiss National Science Foundation under the program CEEC/NIS. One of the authors (A.O.) acknowledges his appreciation for a grant from the Swedish Foundation for International Cooperation in Research and Higher Education.



**APPENDIX A**

For our purposes it is convenient to rewrite the set of equations (1) in an equivalent form

$$f_1(E) = 2 \cos \xi, \quad (\text{A1})$$

$$\frac{1}{f_1(E) - f_2^{-1}(E)} = \frac{\sin(N\xi)}{\sin((N+1)\xi)}. \quad (\text{A2})$$

First, let us consider the case of the polyene chain, where the energy is a simple function of  $\xi$ ,

$$E = \pm \sqrt{2(\cosh 2\eta + \cos \xi)}, \quad (\text{A3})$$

and

$$\frac{\sin(N\xi)}{\sin((N+1)\xi)} = C, \quad (\text{A4})$$

$C = -\exp(2\eta)$ . The latter notation is introduced since the asymptotic solutions of (A4), which refer to the band-edge energies, can be found for an arbitrary value of constant  $C$ , not just for its particular value in the Lennard-Jones equation.

For  $C < -1$  the in-band solutions to (A4),  $0 \leq \xi_k \leq \pi$ , satisfy the following inequalities:

$$\frac{\pi k}{N+1} \leq \xi_k \leq \frac{2\pi k}{2N+1}, \quad k = 1, 2, \dots, N, \quad (\text{A5})$$

where  $\xi_1$  ( $\rightarrow 0$  as  $N \rightarrow \infty$ ) and  $\xi_N$  ( $\rightarrow \pi$  as  $N \rightarrow \infty$ ) correspond to the band-edge states. If  $-N/(N+1) < C < 0$ , Eq. (A4) has an imaginary solution for  $\xi_N$  which corresponds to an in-gap (local) state.<sup>26</sup> Such a special situation is not included in the present discussion. (The conditions of local state appearance are the focus of Appendix B.) We note, however, that the asymptotic behavior of solutions to (A4), which determine the band-edge energies and are found for  $C < -1$  (see Eq. (A7)) is also valid for  $C > -1$  (but  $C \neq 0$ ), although the proof of this asymptotic in the latter case is slightly different.

The use of Eq. (A5) allows one to solve Eq. (A4) approximately by using the secant method<sup>27</sup>

$$\xi_k \approx \frac{2\pi k}{2N+1} \times \left[ 1 - \frac{1}{2(N+1)} \frac{(1+C)\sin\left(\frac{\pi k}{2N+1}\right)}{(1+C)\sin\left(\frac{\pi k}{2N+1}\right) - \sin\left(\frac{\pi k}{N+1}\right)} \right]. \quad (\text{A6})$$

Equation (A6) is exact for  $C = -1$  (i.e.,  $\eta = 0$ ). It can easily be verified that the above expression is in a good agreement with the exact (numerical) solutions of Eq. (A4) for  $N \geq 4$  and that the accuracy of this approximation increases very rapidly with the increase of  $N$ .

An important conclusion that follows from Eq. (A6) is that the asymptotic behavior of the band-edge solutions,  $\xi_1$  and  $\xi_N$ , which determine the energies at the band edges, is independent of  $C$ ,

$$\lim_{N \rightarrow \infty} \xi_1 = \frac{\pi}{N}, \quad \lim_{N \rightarrow \infty} \xi_N = \pi - \frac{\pi}{N}, \quad \text{if } C < -1, \quad (\text{A7})$$

and  $\lim_{N \rightarrow \infty} \xi_1 = \pi/N$ ,  $\lim_{N \rightarrow \infty} \xi_N = \pi - \pi/(2N)$ , if  $C = -1$ .

As a consequence, all four band-edge energies of polyene have identical asymptotics,

$$\lim_{N \rightarrow \infty} E_{edge}(N) = E_{edge}(\infty) + \frac{\Delta}{N^2}, \quad (\text{A8})$$

where the values of  $E_{edge}(\infty)$  (assumed  $\neq 0$ ) and  $\Delta$  are determined by the structure of the energy bands. In particular, for the inner band edges (HOMO and LUMO levels of polyene;  $\xi = \pi - \pi/N$ ) we have

$$|E_{edge}(N)| = 2 \sinh |\eta| + \frac{\pi^2}{4N^2 \sinh |\eta|}, \quad (\text{A9})$$

and for the outer band edges we have

$$|E_{edge}(N)| = 2 \cosh \eta - \frac{\pi^2}{4N^2 \cosh \eta}. \quad (\text{A10})$$

Obviously, the only exception of (A8) is the case of zero band gap,  $\eta = 0$  ( $C = -1$ ), when, in accordance with (A3) and (A6), in the limit  $N \rightarrow \infty$ , the HOMO (LUMO) energy behaves as  $N^{-1}$ . It is also worth mentioning that, if the band gap is small ( $|\eta| \ll 1$ ) but finite, the use of asymptotic dependence (A7) in the dispersion law (A3) reveals the existence of intermediate asymptotics:  $E_{LUMO} = -E_{HOMO} \sim N^{-1}$  in the region  $N \gg 1$  but  $|\eta|N \ll \pi$ , which is replaced by the true asymptotics (A9) at  $|\eta|N \gg \pi$ . The latter observation is in good agreement with numerical results presented in Figs. 2 and 3, which show that the larger the band gap, the better the approximation (5), i.e., the  $N^{-2}$  law is “switching on” at smaller values of  $N$ .

The example presented above highlights the following: (i) the values of  $\xi$ , which determine the band-edge energies, approach their limiting values 0 or  $\pi$  as  $N^{-1}$ ; as a consequence, the energies of edge states have the asymptotics of the kind (A8) if the neighboring bands remain separated in the limit  $N \rightarrow \infty$ ; (ii) in the case of zero gap (band joining) the asymptotic behavior of band-edge energy changes qualitatively and becomes  $\sim N^{-1}$ . Now we prove these two statements in the general case.

For energies near the band edges and  $N \gg 1$  Eq. (A2) can be represented in the form

$$\frac{1}{f_1(E_{edge}(\infty)) - f_2^{-1}(E_{edge}(\infty))} + \varepsilon(N) = \frac{\sin(N\xi)}{\sin((N+1)\xi)}, \quad (\text{A11})$$

where

$$\lim_{N \rightarrow \infty} \varepsilon(N) = 0, \quad (\text{A12})$$

and  $E_{edge}(\infty)$  is one of the solutions to Eq. (A1) with  $\xi=0$  or  $\xi=\pi$ . Correspondingly, we are seeking only for those solutions to Eq. (A11) that determine the values of  $\xi$  for the edge states in the long chain limit,  $\xi=\delta$  or  $\xi=\pi-\delta'$ , and satisfy the condition

$$\lim_{N \rightarrow \infty} \delta = 0, \quad \lim_{N \rightarrow \infty} \delta' = 0. \quad (\text{A13})$$

Note that the function  $1/[f_1(E)-f_2^{-1}(E)]$  is a polynomial that takes zero values at the monomer energies. Therefore, the absolute value of the first term on the left-hand side of Eq. (A11) is always non-zero. (Of course, the case of degenerated bands, which has no dependence on  $N$  is excluded.)

In zero approximation, i.e., setting  $\varepsilon(N)=0$ , Eq. (A11) can be solved in exactly the same way as Eq. (A4), so that we obtain

$$\delta = \delta' = \frac{\pi}{N}. \quad (\text{A14})$$

Expanding the left-hand side of Eq. (A1) in powers of  $E-E_{edge}(\infty)$ , and the right-hand side in powers of  $\delta$ , we arrive at (compare with (A8)–(A10))

$$E_{edge}(N) = E_{edge}(\infty) + \frac{\pi^2}{N^2 f_1'(E_{edge}(\infty))} \times \begin{cases} -1, & \text{if } E_{edge}(\infty) \text{ corresponds to } \xi=0, \\ 1, & \text{if } E_{edge}(\infty) \text{ corresponds to } \xi=\pi. \end{cases} \quad (\text{A15})$$

The latter equation implies that  $f_1'(E_{edge}(\infty)) \neq 0$ . If for some of band-edge energies, say, the  $j$ th,  $f_1'(E_{edge}^{(j)}(\infty))=0$ , it means that the neighboring bands join each other at  $E=E_{edge}^{(j)}$ . Indeed, the equation for the band-edge energies  $f_1(E) \pm 2=0$  can be represented in the form

$$\mathcal{P}^{-1}(E)(E-E_{edge}^{(1)})(E-E_{edge}^{(2)}) \dots (E-E_{edge}^{(j)})^2 \dots (E-E_{edge}^{(N_M-1)})=0, \quad (\text{A16})$$

where  $N_M$  is the number of non-degenerated bands in the given oligomer, and  $\mathcal{P}(E)$  is a polynomial, whose degree is less than  $N_M$ . Thus, in such a case, expanding the left-hand side of (A1) in powers of  $E-E_{edge}^{(j)}$  we have to retain the second order term. Then, instead of (A15) we obtain

$$E(N) = E_{edge}(\infty) + \frac{\sqrt{2}\pi}{N \sqrt{|f_1''(E_{edge}(\infty))|}} \times \begin{cases} -1, & \text{if } E_{edge}(\infty) \text{ corresponds to } \xi=0, \\ 1, & \text{if } E_{edge}(\infty) \text{ corresponds to } \xi=\pi. \end{cases} \quad (\text{A17})$$

Thus, in conjugated oligomers of the type  $M-M-\dots-M$  the dependence of band-edge energies on the chain length is characterized by universal asymptotic behavior:

$$\lim_{N \rightarrow \infty} |E_{edge}(N) - E_{edge}(\infty)| \sim N^{-2}, \quad (\text{A18})$$

if the bands are separated, and

$$\lim_{N \rightarrow \infty} |E_{edge}(N) - E_{edge}(\infty)| \sim N^{-1} \quad (\text{A19})$$

in the case of band joining. This result survives as long as the model Hamiltonian used remains applicable.

## APPENDIX B

In general, two qualitatively different cases of asymptotic behavior of the 0-0 transition excitation energy as a function of the oligomer length should be distinguished:

- (i)  $\lim_{N \rightarrow \infty} \Delta_{HL}(N) = \text{const}$  as is assumed in the text; and
- (ii)  $\lim_{N \rightarrow \infty} \Delta_{HL}(N) = 0$ .

The zero limit is realized due to the HOMO and LUMO states approaching each other as  $N \rightarrow \infty$ . These states can be either band-like states or in-gap states. In the former, the zero limiting value of  $\Delta_{HL}$  is due to joining the upper valence and lower conduction bands, whereas in the latter these bands remain separate.

Suppose first that in the limit  $N \rightarrow \infty$  there are no discrete (local) levels between the highest filled and lowest unfilled bands. According to Eq. (1), at the band edges,  $\xi=0, \pi$ , the following equations must be satisfied:  $f_1(E) \pm 2=0$  and  $|f_2(E)|=1$ . Since in the infinite chain limit there are no differences in the band structure of oligomers  $M-M-\dots-M$  and  $M-M-\dots-M-M_1$ , for both types of oligomers the equations just indicated can be rewritten as

$$G_{l,l}^M(E)G_{r,r}^M(E)=0, \quad (\text{B1})$$

and

$$|G_{l,r}^M(E)|=1. \quad (\text{B2})$$

Thus, if in the energy interval of interest there exists *only one solution* to Eq. (B1), substituting this solution into Eq. (B2) gives the necessary and sufficient condition of joining the bands; see examples below.

Using Eq. (1), it is easy to show that in the limit  $N \rightarrow \infty$ , the energies of discrete states (if there are any in the polymer  $\pi$  electron spectrum) must obey the following equation:

$$1 - f_1(E)f_2(E) + f_2^2(E) = 0. \quad (\text{B3})$$

In the case of oligomers  $M-M-\dots-M$ , i.e., under the substitution of expressions of  $f_1(E)$  and  $f_2(E)$  from Eq. (2), Eq. (B3) takes the form of Eq. (B1). For  $M_1-M_2-M_1-\dots-M_2-M_1$  we have instead of (B1)

$$\begin{aligned} & (G_{l,r}^{M_2}(E))^2 + [G_{l,l}^{M_2}(E)G_{r,r}^{M_2}(E) - (G_{l,r}^{M_2}(E))^2] \\ & \times [1 - G_{l,l}^{M_1}(E)G_{r,r}^{M_2}(E) - G_{l,l}^{M_2}(E)G_{r,r}^{M_1}(E)] \\ & + G_{l,l}^{M_1}(E)G_{r,r}^{M_1}(E)[G_{l,l}^{M_2}(E)G_{r,r}^{M_2}(E) \\ & - (G_{l,r}^{M_2}(E))^2] = 0. \end{aligned} \quad (\text{B4})$$

It also can be proved that at the energy of discrete states

$$|G_{l,r}^M(E)| > 1, \quad (\text{B5})$$

and

$$\left| \frac{G_{l,r}^{M_1}(E)}{G_{l,r}^{M_2}(E)} [G_{l,l}^{M_2}(E)G_{r,r}^{M_2}(E) - (G_{l,r}^{M_2}(E))^2] \right| > 1, \quad (\text{B6})$$

for the first and second types of oligomers under consideration, respectively.

The condition for the existence of in-gap states follows from the substitution of the solution to Eq. (B1) (or (B4)) into Eq. (B5) (or (B6)). If such a state does exist, the  $N^{-2}$  law of HOMO-LUMO gap decrease is no longer valid.

To utilize the general conditions of band joining and of the existence of local states formulated above, one needs the explicit expressions of monomer Green functions that are in Eqs. (B1)–(B6). For the oligomers of focus these are vinylene, phenylene, and phenylenevinylene groups. Finding the matrix elements of the operator  $(E - H^M)^{-1}$ , where  $H^M$  is the Hückel Hamiltonian of the above indicated groups in its conventional representation,<sup>28</sup> is straightforward and gives ( $E$  is in units of  $\beta$ )

$$G_{l,l}^M(E) = G_{r,r}^M(E) = \frac{E \exp(-\eta)}{E^2 - \exp(2\eta)}, \quad (\text{B7})$$

$$G_{l,r}^M(E) = \frac{1}{E^2 - \exp(2\eta)},$$

M—vinylene;

$$G_{l,l}^M(E) = G_{r,r}^M(E) = \frac{E[E^2 - 2\gamma^2 \cosh(2\eta_{ph}) - \gamma^2]}{(E^2 - 4\gamma^2 \cosh^2 \eta_{ph})[E^2 - \gamma^2(2\cosh(2\eta_{ph}) - 1)]},$$

$$G_{l,r}^M(E) = \frac{2\gamma^3 \cosh(\eta_{ph})}{(E^2 - 4\gamma^2 \cosh^2 \eta_{ph})[E^2 - \gamma^2(2\cosh(2\eta_{ph}) - 1)]}, \quad (\text{B8})$$

M—phenylene (aromatic geometry);

$$G_{l,l}^M(E) = G_{r,r}^M(E) = \frac{E[E^2 - \gamma^2 \exp(2\eta_{ph}) - 2\gamma^2 \exp(-2\eta_{ph})]}{[E^2 - 2\gamma^2 \exp(-2\eta_{ph})]^2 - \gamma^2 \exp(2\eta_{ph})E^2},$$

$$G_{l,r}^M(E) = \frac{2\gamma^3 \exp(-\eta_{ph})}{[E^2 - 2\gamma^2 \exp(-2\eta_{ph})]^2 - \gamma^2 \exp(2\eta_{ph})E^2}, \quad (\text{B9})$$

M—phenylene (quinoid geometry);

$$\mathcal{G}_{l,l}^M(E) = \exp(-\eta)E\{[E^2 - \gamma^2 \exp(2\eta_{ph}) - 2\gamma^2 \exp(-2\eta_{ph})][E^2 - \exp(2\eta)] - \exp(-2\eta)[E^2 - \gamma^2 \exp(2\eta_{ph})]\},$$

$$\mathcal{N}(E)G_{r,r}^M(E) = \exp(-\eta)E\{[E^2 - 2\gamma^2 \exp(-2\eta_{ph})^2 - \gamma^2 \exp(2\eta_{ph})E^2 - \exp(-2\eta)[E^2 - 2\gamma^2 \exp(-2\eta_{ph}) - \gamma^2 \exp(2\eta_{ph})]\}, \quad (\text{B10})$$

$$\mathcal{N}(E)G_{l,r}^M(E) = 2\gamma^3 \exp(-(\eta + \eta_{ph})),$$

where

$$\mathcal{N}(E) = \{[E^2 - 2\gamma^2 \exp(-2\eta_{ph})]^2 - \gamma^2 \exp(2\eta_{ph})E^2\} \times [E^2 - \exp(2\eta)] - \exp(-2\eta)E^2[E^2 - \gamma^2 \exp(2\eta_{ph}) - 2\gamma^2 \exp(-2\eta_{ph})], \quad (\text{B11})$$

M—phenylenevinylene.

In the above equations, parameter  $\eta$  distinguishes short and long C-C bonds in the polyene chain (Eq. (B7)) and between phenyl rings (Eqs. (B10) and (B11)); parameter  $\eta_{ph}$  has a similar meaning but with respect to C-C bonds within the rings, while parameter  $\gamma$  accounts for the difference in electron transfer interaction within and between phenyl rings. A more detailed definition of the characteristic parameters is given in the body of the text; see also Fig. 1. The Green functions (B10) refer to the aromatic ( $\eta_{ph} = 0$ ,  $\eta > 0$ ) and quinoid ( $\eta_{ph} \neq 0$ ,  $\eta < 0$ ) structure of the PPV backbone.

The equations for the Green function matrix elements just presented complete the definition of explicit expressions of functions  $f_1(E)$  and  $f_2(E)$  for the specific cases of polyene, polyparaphenylene, and polyparaphenylenevinylene oligomers discussed in this article.

It should be emphasized that according to the Green function definition the eigenvalues of the monomer Hamiltonian, which correspond to zero amplitudes of the wave function at the  $l$ th or  $r$ th site or both, are not present among poles of the Green function matrix elements which refer to the sites indicated. Therefore, apart from the four  $\pi$  electron levels defined in Eqs. (B8) and (B9), the phenyl spectrum contains two additional levels at energies  $E = \pm \gamma \sqrt{2 \cosh(2\eta_{ph}) - 1}$  (which are doubly degenerate, see Eq. (B8)) in the case of the aromatic structure of the ring, and  $E = \pm \gamma \exp \eta_{ph}$  (which are non-degenerate) in the case of the quinoid structure. The former correspond to states with a node at the  $l$  or  $r$  site, whereas the latter corresponds to states with two nodes at these same sites. Just this one difference between monomer electron states gives rise to the qualitative difference of the band structure of PPP with aromatic and quinoid geometries of the backbone; see Appendix C.

Similar to the  $\pi$  electron spectrum of the phenyl ring, the spectrum of the phenylenevinylene group determined by poles of the Green functions (B10) is not complete and two

levels (with energies  $E = \pm \gamma \exp \eta_{ph}$ ) should be added. These levels correspond to states with nodes at the  $l$ th and  $r$ th sites of phenylene and vinylene and are not split therefore by the intermonomer interaction. And again, similar to PPP oligomers, in the case of aromatic-like geometry one can expect an increase in the number of bands in the PPV spectrum due to the bond alternation within the phenyl ring.

Now we turn to the question of whether the HOMO-LUMO gap of the oligomers of focus can be zero in the limit  $N \rightarrow \infty$ , and if yes, is this due to the conduction and valence bands joining or due to the existence of local states.

It should be mentioned first that for the type of oligomers given the gap closing can occur only at zero energy—the on-site energy of carbon. Taking into account the definition of the Green function components, it is easy to see that both Eq. (B1) and Eq. (B4) have the solution  $E=0$ . Substituting this value into Eqs. (B2), (B5), and (B6) it can be concluded that the HOMO-LUMO gap closing due to joining the lowest conduction and the highest valence bands or due to the existence of a twofold degenerated discrete level in the middle of the gap takes place under the following conditions:

$$\eta \leq 0, \quad \gamma^{-1} \geq 2(2 \cosh(2 \eta_{ph}) - 1) \cosh \eta_{ph}, \quad (\text{B12})$$

$$\gamma^{-1} \geq 2 \exp(-3 \eta_{ph}),$$

and

$$\gamma^{-1} \geq 2 \exp(3(\eta - \eta_{ph}))$$

in polyenes, the benzenoid form of PPP, the quinoid form of PPP, and PPV, respectively.

The above relations make it apparent of that the band gap depends on the geometry of oligomer backbone. In particular, it is seen that the anomalously narrow band gap of PPV given in Table I at  $\gamma=1$ ,  $\eta_{ph} = -\eta=0.1$  was indeed to be expected.

## APPENDIX C

Here we derive equations that determine the  $\pi$  electron energy spectrum of the minimal length ( $N=2$ ) and infinite oligomers of polyene, polyparaphenylene (in quinoid and benzenoid forms), and polyparaphenylenevinylene.

By substituting explicit expressions of  $f_1(E)$  and  $f_2(E)$  in Eq. (7), we obtain

$$1 - G_{l,l}^M(E) G_{r,r}^M(E) = 0 \quad (\text{C1})$$

and

$$1 - G_{l,l}^{M_1}(E) G_{r,r}^{M_2}(E) - G_{l,l}^{M_2}(E) G_{r,r}^{M_1}(E) + G_{l,l}^{M_1}(E) G_{r,r}^{M_1}(E) [G_{l,l}^{M_2}(E) G_{r,r}^{M_2}(E) - (G_{l,r}^{M_2}(E))^2] = 0, \quad (\text{C2})$$

which are the secular equations for molecules  $M-M$  and  $M_1-M_2-M_1$ , respectively.

If  $G_{l,l}^M(E) = G_{r,r}^M(E)$ , as is the case in vinylene and phenylene, the above equations can be rewritten in a more simple form. Specifically, Eq. (C1) would read

$$1 + G_{l,l}^M(E) = 0, \quad (\text{C1a})$$

$$1 - G_{l,l}^M(E) = 0,$$

and Eq. (C2) takes the form

$$1 - G_{l,l}^{M_1}(E) (G_{l,l}^{M_2}(E) + G_{l,r}^{M_2}(E)) = 0, \quad (\text{C2a})$$

$$1 - G_{l,l}^{M_1}(E) (G_{l,l}^{M_2}(E) - G_{l,r}^{M_2}(E)) = 0.$$

The continuous spectrum of infinite oligomers is determined by

$$f_1(E) - 2 \cos \xi = 0, \quad (\text{C3})$$

where, again, for the oligomers under consideration the expression of function  $f_1(E)$  can be simplified in a similar way. Note also that, since the perturbation of band states by a local defect goes to zero as  $N \rightarrow \infty$ , one can use the definition of  $f_1(E)$  given in Eq. (2) for determining the dispersion law of both types of oligomers.

## 1. Polyenes

For polyenes finding solutions to Eqs. (C1a) and (C3) with the Green functions defined in (B7) is elementary, so for the HOMO-LUMO gap ( $= 2|E_{LUMO}|$ ) we have

$$\Delta_{HL}(2) = \exp(-\eta) (\sqrt{4 \exp(4\eta) + 1} - 1), \quad (\text{C4})$$

$$\Delta_{HL}(\infty) = 4 \sinh |\eta|.$$

## 2. Polyparaphenylenes

Taking the definitions of the Green functions (B8) and (B9) into account, it is easy to see that, due to  $G_{l,l}^M(E) = -G_{l,l}^M(-E)$  for both benzenoid and quinoid geometries of phenyl ring, two equations (C1a) have the same form. So, the non-degenerated  $\pi$  electron levels of diphenyl  $\pm E_{1-4}$  correspond to the roots of the following equation:

$$E^4 + E^3 - \gamma^2 [4 \cosh(2 \eta_{ph}) + 1] E^2 - \gamma^2 [2 \cosh(2 \eta_{ph}) + 1] E + 2 \gamma^4 [2 \cosh(2 \eta_{ph}) - 1] [\cosh(2 \eta_{ph}) + 1] = 0 \quad (\text{C5})$$

for benzenoid-like structure, and

$$E^4 + E^3 - \gamma^2 [\exp(2 \eta_{ph}) + 4 \exp(-2 \eta_{ph})] E^2 - \gamma^2 [\exp(2 \eta_{ph}) + 2 \exp(-2 \eta_{ph})] E + 4 \gamma^4 \exp(-4 \eta_{ph}) = 0 \quad (\text{C6})$$

for quinoid structure.

Corresponding to this, the HOMO-LUMO gap of diphenyl is determined by the smallest of these roots in the absolute value. For a number of parameters  $\eta_{ph}$  and  $\gamma$  the values of  $\Delta_{HL}(2)$  of diphenyl are presented in Table I.

It is interesting to note that as seen from the phenyl ring symmetry,  $N=2$  is the only case where PPP oligomers of the benzenoid- and quinoid-like structures have the equal number of split  $\pi$  electron levels. For  $N \geq 3$  there are  $6N$  non-degenerate states in the case of benzenoid-like geometry, and  $4N$  non-degenerate and two  $N$ -fold degenerate states in the case of quinoid-like geometry. In the infinite chain limit, we

obtain equations of the third and second order in powers  $E^2$  which determine the  $\pi$  electron bands of the former and latter structures, respectively.

Precisely six bands of the benzenoid-like PPP can be defined as  $E_{1-6}(N \rightarrow \infty, \xi) = \pm \sqrt{Z + \gamma^2(2 \cosh(2\eta_{ph}) - 1)}$ , where  $Z$  is a solution to

$$E_{1-4}(N \rightarrow \infty, \xi) = \pm \frac{1}{\sqrt{2}} \{1 + \gamma^2 \exp(2\eta_{ph}) + 4\gamma^2 \exp(-2\eta_{ph}) \pm \sqrt{[1 - \gamma^2 \exp(2\eta_{ph})]^2 + 8\gamma^2 \exp(-2\eta_{ph}) [1 + \gamma^2 \exp(2\eta_{ph}) + 2\gamma \exp \eta_{ph} \cos \xi]^2}\}^{1/2}. \quad (C8)$$

(the latter equation has been reported previously).<sup>3</sup>

The minimal positive value of roots  $E_{1-6}(N \rightarrow \infty, 0)$  and  $E_{1-4}(N \rightarrow \infty, 0)$  determines the band bottom of the lowest conduction band of the benzenoid and quinoid form of PPP, respectively, and thus, the value of  $\Delta_{HL}(\infty)$ , as defined in Eqs. (10), (11), and (12).

### 3. Polyparaphenylenevinylenes

The substitution of the vinylene and phenylene group Green functions defined in Eqs. (B7) and (B8) in Eq. (C2a) yields

$$E^5 \pm \exp(\eta)E^4 - [4\gamma^2 \exp(-2\eta_{ph}) + \gamma^2 \exp(2\eta_{ph}) + \exp(-2\eta)]E^3 \mp \gamma^2 \exp(\eta)[4 \exp(-2\eta_{ph}) + \exp(2\eta_{ph})]E^2 + \gamma^2[4\gamma^2 \exp(-4\eta_{ph}) + \exp(-2\eta)(\exp(2\eta_{ph}) \pm 2 \exp(-2\eta_{ph}))]E - 4\gamma^4 \exp(\eta - 4\eta_{ph}) = 0, \quad (C9)$$

where the upper and lower signs correspond to the upper and lower equations in (C2a), respectively.

Equation (C9) (with both signs) determines the position of 10 non-degenerate  $\pi$  electron levels of stilbene. (There are also two twofold degenerate levels with energies equal to  $\pm \gamma \exp \eta_{ph}$ .) It can be shown that  $E_{LUMO}$  is one of the solutions to Eq. (C9) and has the lower sign in it. This solution was used to obtain values of the HOMO-LUMO gap of stilbene shown in Table I.

By substituting the Green function (B10) in (C3) with function  $f_1(E)$  defined in Eq. (2) we obtain

$$E^6 - [\gamma^2(4 \exp(-2\eta_{ph}) + \exp(2\eta_{ph}) + 2 \cosh(2\eta) + \exp(-2\eta))]E^4 + \{\exp(-4\eta) + \gamma^2[4 \exp(-2\eta_{ph})(\gamma^2 \exp(-2\eta_{ph}) + 2 \cosh(2\eta)) + \exp(2\eta_{ph})(2 \cosh(2\eta) + \exp(-2\eta))]\}E^2 - \gamma^2[\exp(2\eta_{ph} - 4\eta) + 4\gamma^2 \exp(2\eta - 4\eta_{ph}) + 4\gamma \exp(-(\eta_{ph} + \eta)) \cos \xi] = 0. \quad (C10)$$

From the above equation one can easily derive an ana-

$$Z^3 - (1 + 3\gamma^2)Z^2 - 4\gamma^2[\gamma \cosh(2\eta_{ph}) \cos \xi + \sinh^2 \eta_{ph}]Z + 4\gamma^4 \sinh^2 \eta_{ph} = 0. \quad (C7)$$

The above equation results from Eq. (C3) after substituting the explicit expressions of the Green functions (B8). The four bands of quinoid-like PPP are determined by

lytical expression of the dispersion law of three valence (or symmetrical conduction) bands of PPV as a function of parameters characteristic of the structure. Note in this connection that at  $\xi = \pi$  three roots of Eq. (C10) (that is, of Eq. (13) in the body of the text)  $|E_1| \leq |E_2| \leq |E_3|$  determine the bottom of the first ( $|E_1|$ ) and third ( $|E_3|$ ) conduction bands, and the top of the second conduction band ( $|E_2|$ ), whereas at  $\xi = 0$  these roots give the position of the top of the first and third conduction bands (values of  $|E_1|$  and  $|E_3|$ , respectively), and of the bottom of the second band.

Thus, the proposed formalism allows one to find the expression of band energies of quite complex polymers in an analytical form. To our knowledge, Eqs. (C7) and (C10), which determine the band structure, respectively, of PPP (where the aromatic-like geometry is mimicked by alternating bonds within phenyl rings) and PPV are presented here for the first time.

<sup>1</sup>I. D. W. Samuel, I. Ledoux, C. Dhenaut, J. Zyss, H. H. Fox, R. R. Schrock, and R. J. Silbey, *Science* **265**, 1070 (1994).

<sup>2</sup>J. L. Brédas, *J. Chem. Phys.* **82**, 3808 (1985).

<sup>3</sup>C. Ambrosch-Draxl, J. A. Majewski, P. Vogl, and G. Leising, *Phys. Rev. B* **51**, 9668 (1995).

<sup>4</sup>B. E. Kohler, *J. Chem. Phys.* **93**, 5838 (1990).

<sup>5</sup>G. G. Dyadyusha, V. M. Rozenbaum, and M. L. Dekhtyar, *Zh. Eksp. Teor. Fiz.* **100**, 1051 (1991).

<sup>6</sup>B. E. Kohler, L. I. Malysheva, and A. I. Onipko, *J. Chem. Phys.* **103**, 6068 (1995).

<sup>7</sup>L. I. Malysheva and A. I. Onipko, *Synth. Met.* **80**, 11 (1996); *J. Chem. Phys.* **105**, 11 032 (1996).

<sup>8</sup>B. E. Kohler and I. D. W. Samuel, *J. Chem. Phys.* **103**, 6248 (1995).

<sup>9</sup>B. E. Kohler and J. C. Woehl, *J. Chem. Phys.* **103**, 6253 (1995).

<sup>10</sup>A. A. Ovchinnikov, I. I. Ukrainskii, and G. F. Kventsel, *Sov. Phys. Usp.* **15**, 575 (1973).

<sup>11</sup>D. Baeriswyl, D. K. Campbell, and S. Mazumdar, in *Conducting Polymers*, edited by H. Kiess (Springer, Berlin, 1990).

<sup>12</sup>B. S. Hudson and B. E. Kohler, *Chem. Phys. Lett.* **14**, 299 (1972).

<sup>13</sup>K. Schulten and M. Karplus, *Chem. Phys. Lett.* **14**, 305 (1972).

<sup>14</sup>Y. Jido, T. Inagaki, and H. Fukutome, *Prog. Theor. Phys.* **48**, 808 (1972).

<sup>15</sup>M. V. Kaulgud and V. H. Chitgopkar, *J. Chem. Soc. Faraday Trans. II* **73**, 1385 (1977).

<sup>16</sup>G. G. Dyadyusha, M. N. Ushomirskii, *Zh. Strukt. Khim.* **28**, 17 (1987).

<sup>17</sup>E. Hückel, *Z. Phys.* **70**, 204 (1931); **76**, 628 (1932).

<sup>18</sup>R. Schenk, H. Gregorius, K. Meerholz, J. Heinze, and K. Müllen, *J. Am. Chem. Soc.* **113**, 2634 (1991).

- <sup>19</sup>(a) A. Onipko, Yu. Klymenko, and L. Malysheva, *J. Chem. Phys.* **107**, 5032; (b) Yu. Klymenko and A. Onipko (unpublished).
- <sup>20</sup>J. L. Brédas, B. Thémans, J. G. Fripiat, and J. M. André, *Phys. Rev. B* **29**, 6761 (1985).
- <sup>21</sup>W. A. Harrison, *Electronic Structure and the Properties of Solids* (Freeman, San Francisco, 1980).
- <sup>22</sup>J. L. Brédas, *Synth. Met.* **17**, 115 (1987).
- <sup>23</sup>J. M. André, J. Delhalle, and J. L. Brédas, *Quantum Chemistry Aided Design of Organic Polymers* (World Scientific, Singapore, 1991).
- <sup>24</sup>A. D. Kachkovski, *Structure and Color of Polymethine Dyes* (Naukova Dumka, Kiev, 1989) (in Russian).
- <sup>25</sup>N. Tyutyulkov, J. Fabian, A. Mehlhorn, F. Dietz, and A. Tadjer, *Polymethine Dyes. Structure and Properties* (St. Kliment Ohridski University Press, Sofia, 1991).
- <sup>26</sup>L. I. Malysheva and A. I. Onipko, *Synth. Met.* **80**, 11 (1996); *J. Chem. Phys.* **105**, 11 032 (1996).
- <sup>27</sup>J. S. Vandergraft, *Introduction to Numerical Computations* (Academic, New York, 1978).
- <sup>28</sup>A. Streitwieser, Jr., *Molecular Orbital Theory* (Wiley, New York, 1961).